Available online at www.sciencedirect.com
SCIENCE DIRECT®
International Journal of Heat and Fluid Flow 27 (2006) 33–41
International Journal of HEAT AND FLUID FLOW
www.elsevier.com/locate/ijhff

Investigation of the effect of confinement on the heat transfer to round impinging jets exiting a long pipe

N. Gao, D. Ewing *

Department of Mechanical Engineering, McMaster University, Hamilton, Ont., Canada L8S 4L7

Received 29 May 2004; accepted 22 June 2005
Available online 25 August 2005

Abstract

Measurements were performed to characterize the effect that a confining plate had on the heat transfer produced by round turbulent impinging jets exiting a long pipe with Reynolds numbers of 17 000–28 000. It was found that the presence of the confining plate did not have a large impact on the heat transfer produced by the impinging jets with $H/D \geqslant 1$, but did for the jets with $H/D \leqslant 0.5$, reducing the local heat transfer in the region $r/D \geqslant 1.5$ by up to 50%. Measurements of the static and fluctuating wall pressure in the jets indicated that the turbulent fluctuations near the heat transfer surface were reduced in size and convected more slowly in this region for the confined jets with $H/D \leqslant 0.5$. The location of the decrease in the heat transfer and the fluctuating wall pressure in the confined jets shifted laterally outward as the nozzle-to-plate distance increased, and seemed to be associated with the flow reattaching to the confining plate.

Keywords: Forced convection; Impinging jet; Confinement

1. Introduction

Turbulent, round impinging jets are widely used in practical cooling and drying applications and thus, have been the subject of numerous investigations to characterize their heat transfer. Many earlier investigations focused on characterizing the heat transfer produced by unconfined submerged impinging jets (e.g., Baughn and Shimizu, 1989; Goldstein et al., 1990; Yan et al., 1992; Lytle and Webb, 1994). More recently, there has been increased interest in characterizing the heat transfer produced by confined impinging jets, where the impinging jet exits an orifice in a large plate (e.g., Colucci and Viskanta, 1996; Fitzgerald and Garimella, 1997; Brignoni and Garimella, 2000; Lee and Lee, 2000). In both cases, the heat transfer produced by the impinging jets depends on a number of parameters including the distance between the nozzle and heat transfer surface, the jet Reynolds number, and the geometry of the nozzle.

The development of the flow produced by confined impinging jets differs from the flow produced by unconfined impinging jets, in part, because the presence of the confining plate affects the entrainment into the jet and creates a recirculating flow region below the confining plate. Obot et al. (1983) compared the heat transfer produced by confined and unconfined impinging air jets exiting an ASME nozzle and found that the heat transfer produced by the confined jets was smaller for jets with nozzle-to-plate distances of 2–12 diameters. Garimella and Rice (1995) and Fitzgerald and Garimella (1998) examined the flow formed between the plates for confined impinging jets with nozzle-to-plate distances of 2–4 diameters and found there was a recirculating flow region that moved toward the jet centerline as the nozzle-to-plate distance decreased. More recently,

* Corresponding author. Tel.: +1 905 525 9140x27476; fax: +1 905 572 7944.
E-mail address: ewingd@mcmaster.ca (D. Ewing).

0142-727X/$ - see front matter © 2005 Elsevier Inc. All rights reserved.
doi:10.1016/j.ijheatfluidflow.2005.06.002

Nomenclature

D	nozzle diameter, m
F_{pp}	spectrum of the fluctuating pressure, Pa^2/Hz
f	frequency, Hz
H	nozzle-to-plate distance, m
h	heat transfer coefficient, W/m^2 K
k	thermal conductivity, W/m K
Nu	local Nusselt number, hD/k_a
P	static pressure, Pa
p'	fluctuating pressure, Pa
Q	volumetric flow rate, m^3/s
q	heat flux, W/m^2
r	radial coordinate on the surface, m
Re	Reynolds number, UD/v
T	temperature, K
U	average velocity of the pipe flow, $4Q/(\pi D^2)$, m/s
x	spatial coordinate in a Cartesian system, m
y	spatial coordinate in a Cartesian system, m

Greeks

v	kinematic viscosity of air, m^2/s
ρ	density of air, kg/m^3
θ	angular coordinate on the surface, deg.

Subscripts

a	air
b	bottom (heat transfer) wall
conv	convection
elec	local electrical heating
j	jet
rad	radiation
t	top (confining) wall
w	wall

Behnia et al. (1999) compared the heat transfer produced by confined and unconfined impinging jets exiting a long pipe with a Reynolds number 23 000 using a RANS approach with a v^2–f turbulence closure model. This model predicted that the heat transfer produced by the confined and unconfined impinging jets were the same for jets with nozzle-to-plate distances of 2 diameters. However, the heat transfer produced by the confined impinging jets with nozzle-to-plate distances of 0.1 and 0.5 diameters were significantly smaller than that produced by the unconfined jets in the region $r/D \gtrsim 2.0$.

Heretofore, there have not been any experimental investigations comparing the heat transfer produced by confined and unconfined jets exiting the same nozzle for these small nozzle-to-plate distances. Lytle and Webb (1994) examined the heat transfer produced by unconfined impinging jets exiting a long pipe with nozzle-to-plate distances of 0.1–1 diameters. They found that there was an increase in the heat transfer in the stagnation region for these jets with a local maximum at $r/D \approx 0.5$ that seemed to be caused by the acceleration of the flow through the gap between the nozzle outlet and the plate. There was also a significant increase in the secondary off-axis maximum in the heat transfer that appeared to be caused by an increase in the turbulence generated in the jet as it developed. For these small distances, the addition of a confining plate would have an significant effect on the development of the flow and the heat transfer. Moller (1963) and Nakabayashi et al. (2002) characterized the development of flows exiting a long pipe into a channel between two disks, similar to the geometry of confined impinging jets. They observed that the flow exiting the pipe reattached to the confining wall close to the pipe exit in cases where the nozzle-to-plate distance was small. The reattachment location moved toward the jet centerline as the nozzle-to-plate distance decreased and was essentially independent of the jet Reynolds number for Reynolds number greater than 10 000.

The objective of the current investigation was to characterize the effect that the presence of a confining plate has on the heat transfer produced by impinging jets exiting a long pipe. Measurements of the heat transfer were performed for jets with nozzle-to-plate distances of 0.25–6 diameters. The effect of the confining plate on the flow field was also examined using measurements of the static and fluctuating wall pressure in these jets. The experimental facilities used in this investigation are presented in the next section. The results of the experiments are then presented and discussed. Finally, the conclusions of the investigations are presented.

2. Experimental methodology

The heat transfer produced by the impinging jets was measured using the facility shown in Fig. 1, similar to that used in Gao et al. (2003). The jet in this facility exits a round pipe with an inner diameter of 12.7 mm and a length of 96 diameters. The air flow to the pipe from a compressed air line was filtered and then passed through a pressure regulator. The air flow rate was measured using a rotameter and then entered the pipe through a flow straightening device. The mean velocity profiles measured at the pipe exit using hot-wire anemometry for the case of a free jet were in good agreement with the profiles for a fully developed pipe flow.

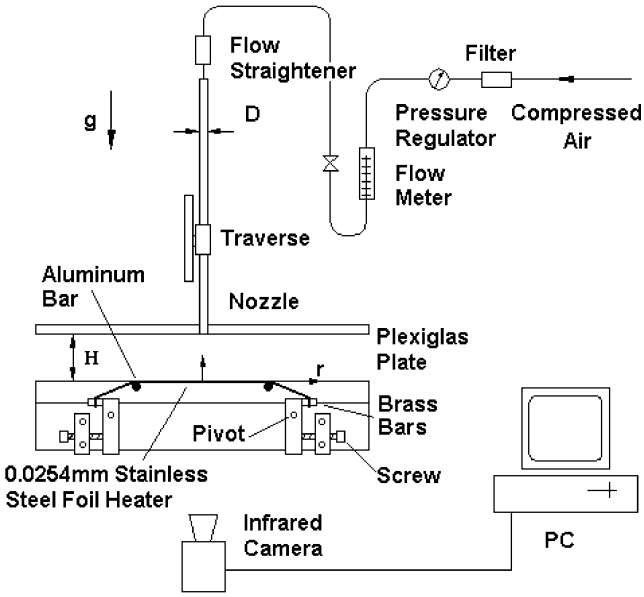

Fig. 1. Schematic of the experimental setup.

The flow exiting the pipe impinged onto a 45.7 cm by 45.7 cm surface mounted perpendicular to the nozzle. The surface contained two plexi-glass plates mounted on an aluminum frame with a 50.8 mm gap between the plates. A 50.8 mm wide, 0.025 mm thick stainless steel foil, that acted as the heat transfer surface was mounted in this gap. The length of the stainless steel foil was shortened for this investigation by mounting two 5 mm diameter aluminum rods across this gap at distances of 90 mm from the jet centerline. The foil was then attached to adjustable aluminum mounts positioned below the surface that were used to tension the foil over the rods. The adjusted mounts were attached to two 50 mm high plexi-glass plates mounted on either side of the gap that also acted to contain the air beneath the heat foil. The remainder of the slot in the top surface was covered using clear tape. The deflection of the stainless steel foil during the experiments was measured using a dial gauge mounted below the foil and it was less than 0.2 mm ($0.016D$) in all cases.

The confined impinging jet was formed by mounting a 40.6 cm by 40.6 cm plexi-glass plate flush with the pipe exit. The long pipe and the confining plate were mounted on a traversing mechanism that was used to change the distance between the nozzle exit and the heat transfer surface. The distance between the nozzle and the foil was measured using a digital caliper attached to this traversing mechanism. The separation distance between the plates for the confined jet measurements was also maintained using machined spacers positioned between the corners of the plates.

The stainless steel foil was heated using a regulated DC power supply that could produce up to 4500 W/m^2 of local electrical heating in the foil. The ends of the foil were clamped to the adjustable aluminum mounts using machined square brass bars that were connected to the power supply using heavy gauge wires. The current through the foil was measured using a meter on the power supply, while the voltage drop across the foil was measured using a multi-meter. The uncertainty in the calculation of the power generated was approximately 1%. The heat transfer losses from the foil during the impinging jet experiments were estimated and it was found that the radiation losses from the foil were the most prominent, reaching up to 5% of the local heating. The losses through the air below the foil was estimated to be less than 1% of the local electrical heating, while the lateral heat conduction in the foil, estimated from the temperature gradients on the foil, was less than 0.4% of the local electrical heating in all cases. The latter two losses were neglected introducing a bias error in the measurements. This was considered in the error analysis.

The local temperature distributions on the bottom of the heated foil were measured using a FLIR THERMACAM SC3000 infrared camera located below the foil. The thermal camera has a resolution of the 0.02 °C and a reported accuracy of 1 °C. The bottom of the foil was coated with candle-soot black paint to increase the emissivity of the surface. An experiment was performed to determine the emissivity of the foil's bottom surface (and effectively calibrate the thermal camera) by mounting the foil on an isothermal surface (Gao et al., 2003). It was found that the bottom of the foil had an emissivity of 0.96 ± 0.01 over the temperature range of interest here. This uncertainty in the emissivity resulted in an uncertainty in the measured temperature of approximately ±0.2 °C. Each temperature distribution reported here was determined by averaging 100 samples of the instantaneous temperature distribution measured at 1 Hz. The standard deviations of the local temperatures computed from these images were less than ±0.2 °C, so the uncertainty in the estimator of the mean should be less than approximately ±0.02 °C.

The local heat transfer coefficient for the impinging jet was determined by subtracting the estimate of the local radiation losses from the electrical heating and using the adiabatic jet temperature as a measure of the jet temperature; i.e.,

$$h = \frac{q_{\text{conv}}}{T_{\text{w}}(r,\theta) - T_{\text{j}}(r,\theta)} = \frac{q_{\text{elec}} - q_{\text{rad}}}{T_{\text{w}}(r,\theta) - T_{\text{j}}(r,\theta)}, \tag{1}$$

where $T_{\text{w}}(r, \theta)$ was the local foil temperature and $T_{\text{j}}(r, \theta)$ was the local adiabatic jet temperature determined when the jet impinged on the unheated surface. Thus, the temperature difference was determined by subtracting measurements performed with the thermal camera reducing the effect of any bias error associated with the individual thermal camera measurements. The local adiabatic jet temperature was uniform to within ±0.2 °C and agreed

with the jet air temperature measured with a thermocouple to within experimental uncertainty.

The uniformity of the heating in the foil was initially checked by measuring the temperature distribution on the foil for modest heating when the foil was not cooled by the jet. The temperature of the foil was found to be uniform to within experimental uncertainty. The local Nusselt number distributions on the surface were also found to be reasonable axisymmetric in all cases. For example, the distributions of the local Nusselt number for the unconfined and confined impinging jets with $H/D = 0.25$ and Reynolds number of 23 000 (the worst case considered here) are shown in Fig. 2. The profiles of the local Nusselt number were determined from the centerline of these local Nusselt number distributions.

The uncertainty in the local Nusselt number and the Reynolds number reported were characterized using the approach outlined in Coleman and Steele (1998). The 95% confidence interval for the Nusselt number and the exit Reynolds number were approximately 9% and 7%, respectively. The heat transfer experiments reported here were also repeated four times to characterize the repeatability of the measurements. The profiles of the local Nusselt number from these experiments were within ±3% for jets with $H/D = 0.25$ and ±2% for jets with $H/D \geqslant 0.38$.

The pressure distributions on the surfaces in the confined and unconfined impinging jets were determined by replacing the top and bottom plates with aluminum plates that were at least 30.5 cm by 30.5 cm in size. The static pressure distributions on both plates were

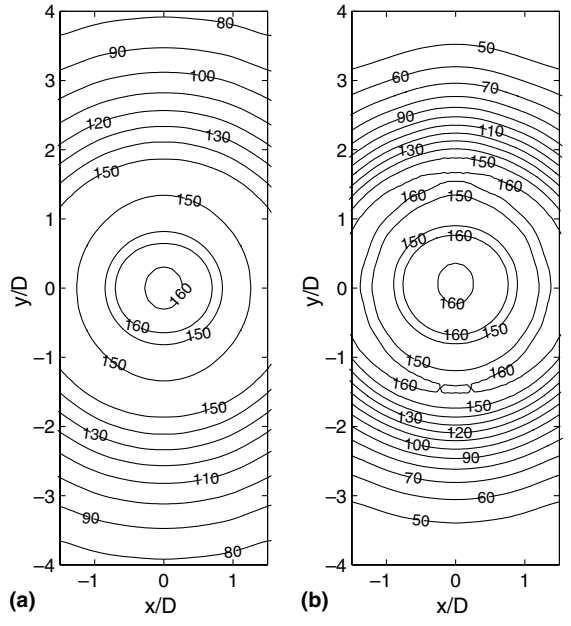

Fig. 2. Distributions of the local Nusselt number for (a) the unconfined jet and (b) the confined jet exiting a long pipe with $H/D = 0.25$ and $Re = 23000$.

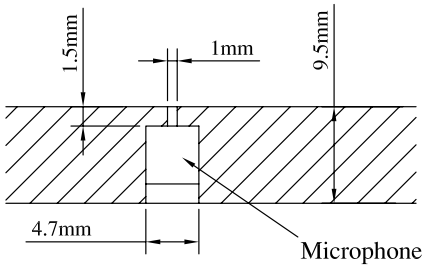

Fig. 3. Schematic of the microphone setup used in the pressure measurements.

measured using arrays of 1.6 mm diameter pressure taps mounted through the walls and a multi-tube bank of oil manometers. The fluctuating wall pressure on the bottom wall was measured using a Sennheiser KE4-211-2 microphone that was mounted into 4.7 mm diameter blind holes machined into the wall to within 1.5 mm of the surface. A 1 mm diameter hole was machined through the remainder of the wall at each location as shown in Fig. 3. The microphone used here had a flat response for frequencies between 20 Hz and 10 000 Hz and the experimentally determined resonance frequency of the sampling system was 8000–9000 Hz, above the frequencies shown here. The microphone was calibrated using a B&K piston phone type 4220 calibrator before the measurements. The voltage signals from the microphone were sampled in 100 blocks of 8192 data points at a frequency of 32 768 Hz using a 14-bit A/D board. The 95% confidence intervals for the static pressure and the variance of the fluctuating pressure were ±5% and ±3–8%, respectively, while the 95% confidence interval for the magnitude of the fluctuating pressure spectra was ±20%.

3. Results and discussion

The profiles of the Nusselt number in the region $r/D \leqslant 4$ for confined and unconfined jets with $H/D = 0.25$–6 and Reynolds number of 23 000 are shown in Fig. 4. The results for the unconfined jet with $H/D = 2$ and 6 agreed with those reported by Baughn and Shimizu (1989) for an unconfined impinging jet exiting a long pipe with the same Reynolds number. The largest discrepancy was less than 5%. The Nusselt numbers for the unconfined jets with $H/D = 0.25$–1 reported here are approximately 15–20% smaller than those reported by Lytle and Webb (1994) for unconfined jets exiting a long pipe with a Reynolds number of 23 000. The Nusselt number for the unconfined jet with $H/D = 6$ reported here and by Baughn and Shimizu (1989) were approximately 15% smaller than those reported by Lytle and Webb (1994). The cause of this difference is not known, but this difference in the previous results was noted by Behnia et al. (1999).

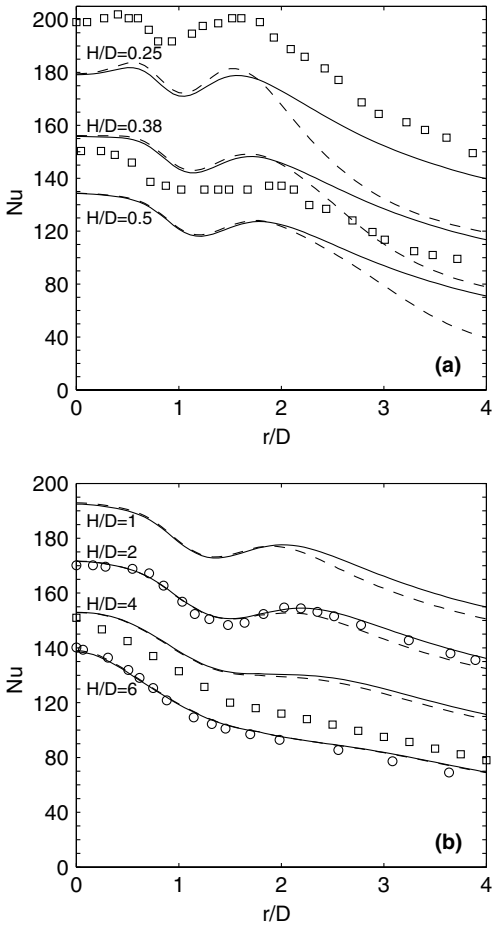

Fig. 4. Profiles of the Nusselt number for (—) the unconfined jets and (- - -) the confined jets with $Re = 23000$. Profiles for the unconfined jets with (○) $H/D = 2$ and 6 and $Re = 23000$ from Baughn and Shimizu (1989) and with (□) $H/D = 0.25$, 0.5, and 6 and $Re = 23000$ from Lytle and Webb (1994).

The presence of the confining plate did not have a large impact on the heat transfer produced by the impinging jets with $H/D \geqslant 1$ in the region $r/D \leqslant 4$ examined here. The presence of the confining plate reduced the heat transfer in the region $r/D > 1.5$ in these cases, but by less than 10% for the jet with $H/D = 1$ and 5% for the jet with $H/D = 4$. The difference decreased with H/D until there was no notable difference for the jet with $H/D = 6$. The presence of the confining plate did have a significant impact on the heat transfer for the impinging jets with $H/D \leqslant 0.5$, particularly in the region $r/D > 1.5$ where the heat transfer was reduced by up to 50%. The increase in the bulk temperature of the air passing through the channel in the confined jets was only on the order of 4% of the difference between the heated wall temperature and the adiabatic jet temperature (or jet temperature). Thus, it was thought that the increase in the bulk temperature of the air was not the cause of the decrease in the heat transfer in the confined jets with $H/D \leqslant 0.5$. The Nusselt number in the confined jets with $H/D \leqslant 0.5$ also decreased relative to that in the unconfined jets over a short distance, suggesting that there was a change in the flow near the wall. The location of this decrease in the heat transfer moved toward the jet centerline as the nozzle-to-plate distance of the jet decreased. Thus, it was thought that it may be associated with the flow reattaching to the confining plate.

The development of the flow fields in the confined and unconfined jets were examined by measuring the distribution of the static and fluctuating pressure on the walls. The distributions of the static pressure on the wall for the confined and unconfined jets with $H/D \leqslant 1$ are shown in Fig. 5. The static pressures presented here are gauge pressures and have been normalized by the dynamic head of the jet, $0.5\rho U^2$, where $U = Q/A$ is the average velocity of the pipe flow. In all cases, there was a maximum in the static pressure at the stagnation point, as expected. The static pressure decreased across the stagnation region in the unconfined impinging jets and approached atmospheric pressure at $r/D \approx 1$. The normalized pressure at the stagnation point in these jets was larger than 1 in part because the centerline velocity of the jet was larger than the average velocity of the pipe flow. The static pressure at the stagnation point also increased when the nozzle-to-plate distance decreased from $H/D = 1$ to 0.25. There was a corresponding increase in the static pressure measured at the pipe entrance. There was little change in either pressure for the jets with $H/D \geqslant 1$. Thus, it was thought that the pressure increase at the stagnation point was due to an increase in the pressure difference required to accelerate the flow through the gap between the nozzle exit and the plate.

The static pressure distributions for the confined impinging jets differed from those for the unconfined jets

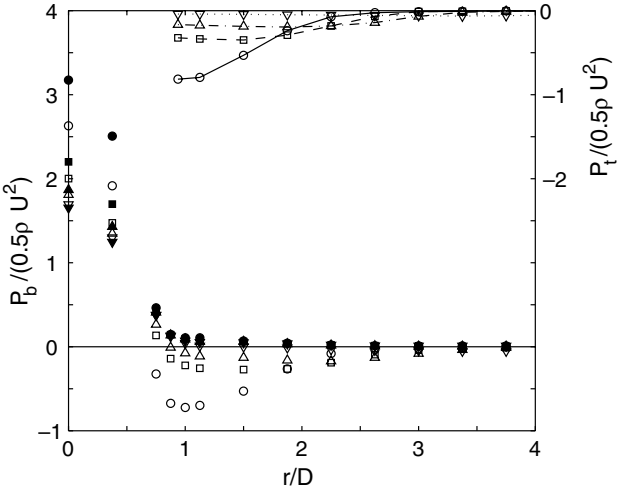

Fig. 5. Profiles of the static wall pressure for the unconfined jets (solid symbols) and the confined jets (open symbols) with H/D: (○) 0.25, (□) 0.38, (△) 0.5, and (▽) 1.0 and $Re = 23000$.

in a number of ways. Most notably, the static pressure on the walls fell below atmospheric pressure in the region $r/D \gtrsim 0.6$. The negative gauge pressures were similar on the top and the bottom walls indicating that the low pressure region was not associated with the turning of the flow. There was also a decrease in the static pressure at the stagnation point similar in magnitude to the minimum in the static pressure, indicating that the presence of the confining plate did not have a large impact on the pressure difference required to accelerate the flow through the gap between the nozzle exit and the bottom plate. The negative gauge pressure in the channel of the confined jet was due to the pressure recovery downstream of the pressure minimum that is normally associated with a deceleration or redistribution of the flow. The location of the minimum in the static pressure shifted outward as the nozzle-to-plate distance increased, and the pressure recovered to atmospheric pressure at $r/D \approx 2.5$ and $r/D \approx 3.5$ for the jets with $H/D = 0.25$ and 0.5, respectively. These locations were in reasonable agreement with the reattachment location determined from the correlation in Nakabayashi et al. (2002) given by[1]

$$\frac{r_R}{D} = 6.45(H/D)^{0.668}, \tag{2}$$

where r_R was the radius where Nakabayashi et al. (2002) observed that the flow reattached to the confining plate. Thus, these results suggest that the increase in the pressure may be associated with the flow attaching to the upper wall.

It is not clear, though, if the pressure recovery and the deceleration of the bulk flow is directly related to the decrease in the heat transfer observed in the wall jet region of the confined impinging jets. In particular, the size of the pressure recovery increased significantly as the nozzle-to-plate distance decreased from $H/D = 0.5$–0.25, whereas the reduction in the heat transfer did not change as much. Lytle and Webb (1994) noted that the increase in the heat transfer observed in the wall region of unconfined jets with small nozzle-to-plate distances seemed to be associated with an increase in turbulent fluctuations in this region. The size of the turbulent fluctuations near the bottom wall in the jets examined here were characterized by measuring the fluctuating pressure on this wall. The standard deviation of the fluctuating wall pressure for the confined and unconfined jets with $H/D = 0.25$ and 0.5, and the corresponding profiles of the Nusselt number are shown in Fig. 6. The fluctuating wall pressure was largest upstream of the secondary peak in the heat transfer and then decreased in the wall jet region. The fluctuating pressure

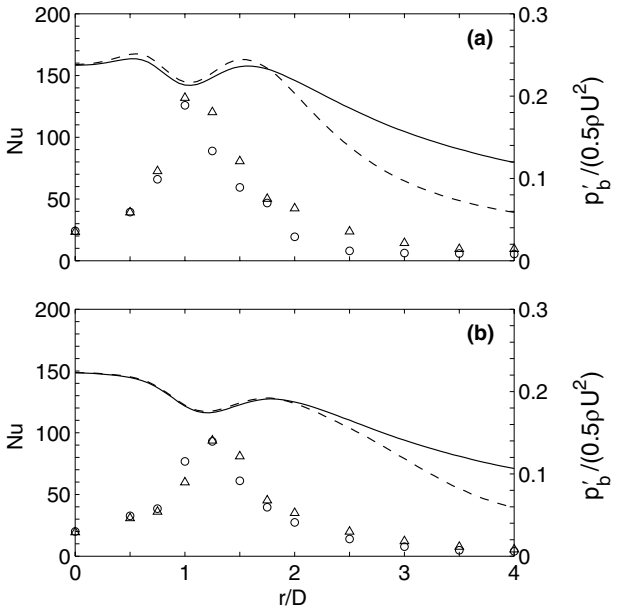

Fig. 6. Comparison of the fluctuating wall pressure and Nusselt number for (△) or (—) the unconfined jets and (○) or (---) the confined jets with (a) $H/D = 0.25$ and (b) $H/D = 0.5$ and $Re = 23000$.

in the wall jet region was smaller in the confined impinging jet indicating there was a reduction in the turbulent fluctuations near the wall.

The frequency spectra of the wall pressure fluctuations for the jets with $H/D = 0.25$ are shown in Fig. 7. The pressure spectra in the two jets are similar in the region $r/D \leqslant 1.0$. There are peaks in the spectra for both jets that correspond to the passage of quasi-periodic large-scale motions in these flows. At $r/D \geqslant 1.5$, the characteristic frequency of the fluctuations in the confined jet are significantly smaller than those in the unconfined jet, likely due to a deceleration of the flow near the wall, consistent with the static pressure measurements. The difference between the pressure spectra in the two jets becomes more significant in the region $r/D \geqslant 2.0$ where the spectra measured for the confined jet are lower in magnitude, particularly at $r/D = 2.5$. This corresponded to the region where the heat transfer produced by the confined jet decreased relative to that for the unconfined jet.

The results are similar for the spectra measured in the jets with $H/D = 0.5$ shown in Fig. 8. The spectra again differed in the region $r/D \geqslant 1.5$. In this case, there is a significant difference in the magnitude of the pressure spectra in the region $r/D \geqslant 3.0$ that corresponds to the region where heat transfer in the confined jet decreased relative to the unconfined jet. The change in the spectra did not occur as rapidly as in the jet with $H/D = 0.25$ and may explain the slower decrease in the heat transfer for the confined jet with $H/D = 0.5$. There was also much less difference between the fluctuating wall pressure spectra for the confined and unconfined impinging

[1] It should be noted that the exponent was reported as 0.0668 in Nakabayashi et al. (2002) but this seems to be a typographical error as the resulting curve did not fit the reported data, whereas 0.668 did.

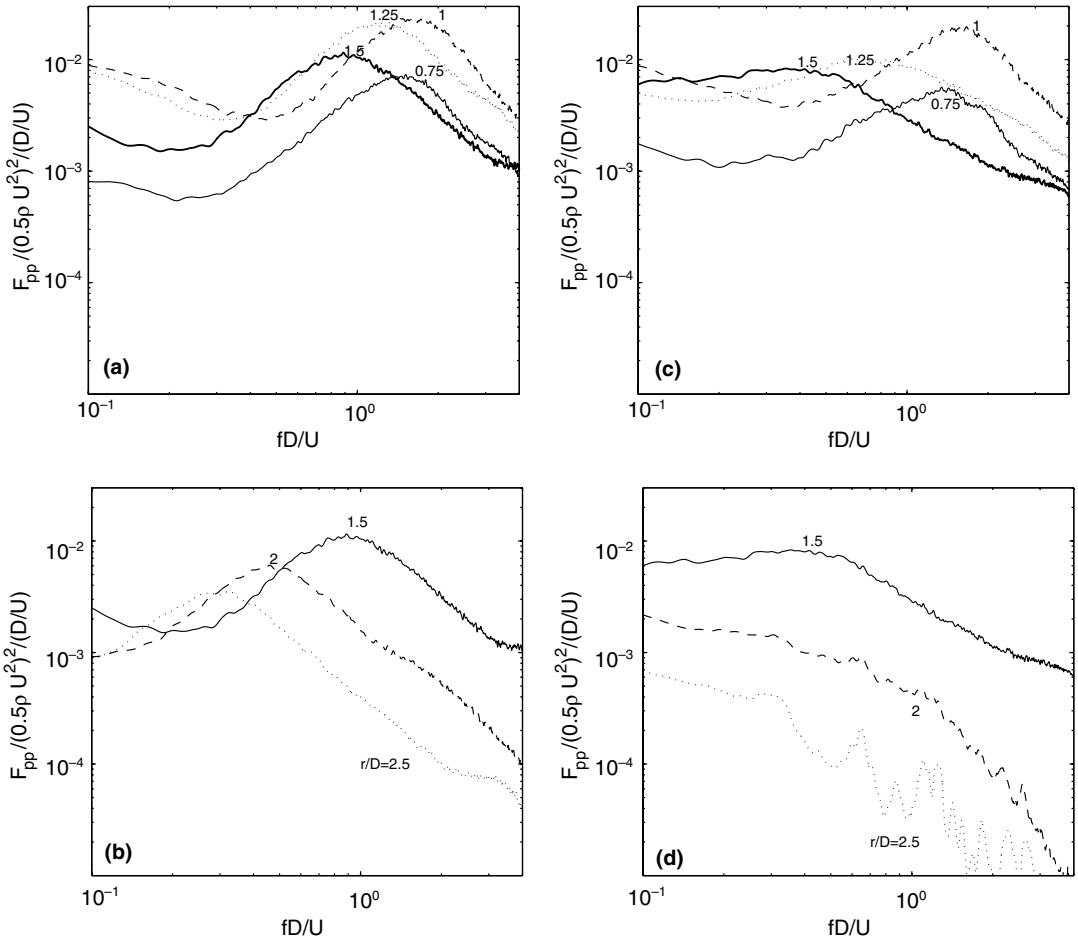

Fig. 7. Spectra of the fluctuating wall pressure at different r/D for (a), (b) the unconfined jet and (c), (d) the confined jet with $H/D = 0.25$ and $Re = 23000$.

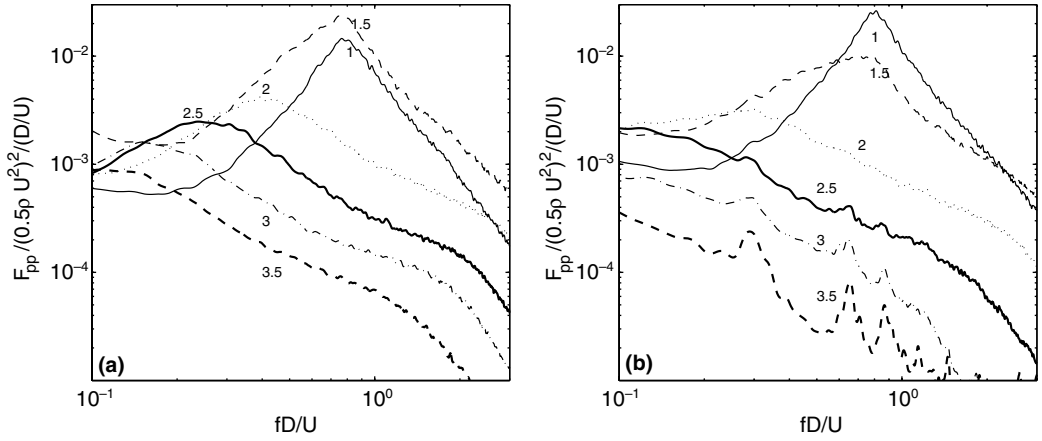

Fig. 8. Spectra of the fluctuating wall pressure at different r/D for (a) the unconfined jet and (b) the confined jet with $H/D = 0.5$ and $Re = 23000$.

jets with $H/D = 1$ shown in Fig. 9. Thus, the results indicate that decrease in the heat transfer observed in the confined jet with $H/D \leqslant 0.5$ was likely due to a decrease (or at least a change) in the turbulent fluctuations near the heat transfer surface that seemed to be associated with the flow reattaching or interacting with the confining plate. This was much less prominent for the jets with $H/D \geqslant 1$ in the region examined here.

The measurements were repeated for impinging jets with Reynolds numbers of 17000 and 28000. The presence of the confining plate had a similar effect on the heat transfer in the wall jet region for all three Reynolds

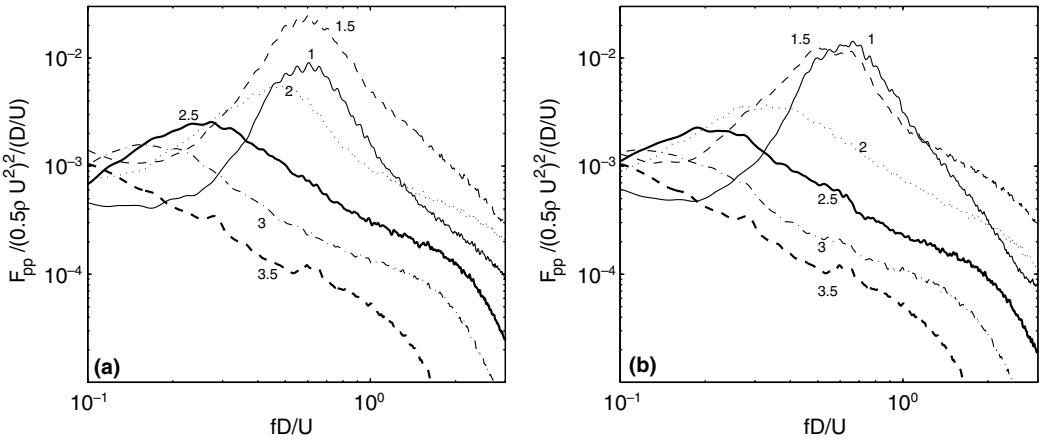

Fig. 9. Spectra of the fluctuating wall pressure at different r/D for (a) the unconfined jet and (b) the confined jet with $H/D = 1.0$ and $Re = 23000$.

numbers. For example, a comparison of the Nusselt number profiles for the jets with $H/D = 0.25$ and 0.5 are shown in Fig. 10. The heat transfer in the wall jet region is reduced by a similar amount for the three Reynolds numbers. In the unconfined jets, the location of the secondary peak in the heat transfer shifted radially outward as the Reynolds number increased, a result that was similar to the measurements of Lytle and Webb (1994). This was less the case in the confined impinging jets. The Reynolds number dependence of the Nusselt number profiles for confined and unconfined jets were similar for the jets with the larger nozzle-to-plate distances but differed for the jets with $H/D = 0.25$. The cause of this difference was not clear from the measurements of the static and fluctuating pressure. Further investigation is required to determine the cause of the change in the Reynolds number dependence of the Nusselt number observed for the confined impinging jets with small nozzle-to-plate distances.

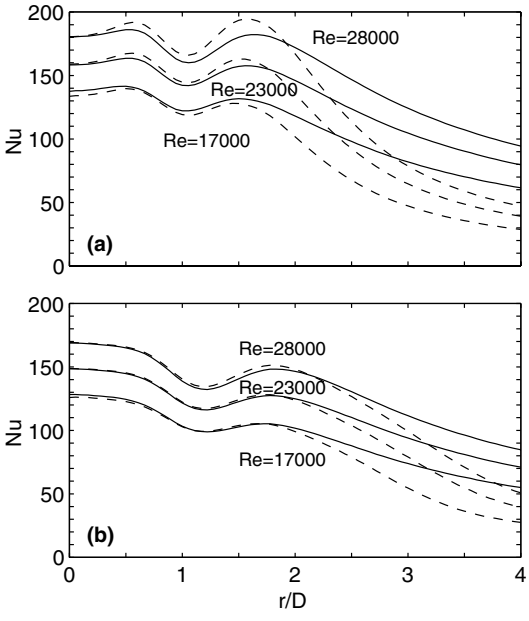

Fig. 10. Profiles of the Nusselt number for (—) the unconfined jets and (- - -) the confined jets with different Reynolds number for (a) $H/D = 0.25$ and (b) $H/D = 0.5$.

4. Summary and concluding remarks

Measurements were performed to examine how the presence of a confining plate affected the heat transfer produced by round, turbulent, impinging jets exiting a long pipe. The presence of the confining plate did not have a significant effect on the heat transfer produced by the impinging jets with $H/D \geqslant 1$, reducing the heat transfer by only up to 10% for the jet with $H/D = 1$. The size of this difference decreased as H/D increased until there was no notable difference in the heat transfer produced by the jets with $H/D = 6$. The presence of the confining plate did have a significant effect on the heat transfer produced by impinging jets with $H/D \leqslant 0.5$, reducing the heat transfer in the region $r/D > 1.5$ by up to 50%. In these cases, the heat transfer produced by the confined impinging jet decreased relative to that produced by the unconfined jet over a short distance, indicating that there was a change in the turbulent flow near the wall.

The development of the flows in the impinging jets were examined using measurements of the static and fluctuating wall pressure. It was found that there was a region of negative static gauge pressure on the walls of the confined jets with $H/D \leqslant 1$ that appeared to be caused by a pressure recovery as the flow reattached to the confining surface. There was also a significant reduction in the magnitude of the wall pressure fluctuations in this region for the confined jets with $H/D \leqslant 0.5$ that was not observed in the jets with $H/D \geqslant 1$. The decrease in the wall pressure fluctuations in the confined jets corresponded to the regions where the heat transfer to the confined impinging jets decreased relative to the

unconfined jets suggesting that the decrease in the heat transfer observed to the confined impinging jets with $H/D \leqslant 0.5$ was caused by a decrease (or at least a change) in the turbulent fluctuations near the heat transfer surface. The location of the decrease in the heat transfer and the fluctuating wall pressure in the confined jets shifted laterally outward as the nozzle-to-plate distance increased, and seemed associated with the flow reattaching to the confining plate.

Acknowledgements

The authors wish to acknowledge the support of the Natural Sciences and Engineering Research Council of Canada and the assistance of Ms. L.C. Ofiara in the preparation of this paper.

References

Baughn, J.W., Shimizu, S., 1989. Heat transfer measurements from a surface with uniform heat flux and an impinging jet. Journal of Heat Transfer 111, 1096–1098.

Behnia, M., Parneix, S., Shabany, Y., Durbin, P.A., 1999. Numerical study of turbulent heat transfer in confined and unconfined impinging jets. International Journal of Heat and Fluid Flow 20, 1–9.

Brignoni, L.A., Garimella, S.V., 2000. Effects of nozzle-inlet chamfering on pressure drop and heat transfer in confined air jet impingement. International Journal of Heat and Mass Transfer 43, 1133–1139.

Coleman, H.W., Steele, W.G., 1998. Experimentation and Uncertainty Analysis for Engineers, second ed. John Wiley, New York.

Colucci, D.W., Viskanta, R., 1996. Effect of nozzle geometry on local convective heat transfer to a confined impinging air jet. Experimental Thermal and Fluid Science 13, 71–80.

Fitzgerald, J.A., Garimella, S.V., 1997. Flow field effects on heat transfer in confined jet impingement. Journal of Heat Transfer 119, 630–632.

Fitzgerald, J.A., Garimella, S.V., 1998. A study of the flow field of a confined and submerged impinging jet. International Journal of Heat Mass Transfer 41, 1025–1034.

Gao, N., Sun, H., Ewing, D., 2003. Heat transfer to impinging round jets with triangular tabs. International Journal of Heat and Mass Transfer 46, 2557–2569.

Garimella, S.V., Rice, R.A., 1995. Confined and submerged liquid jet impingement heat transfer. Journal of Heat Transfer 117, 871–877.

Goldstein, R.J., Sobilik, K.A., Seol, W.S., 1990. Effect of entrainment on the heat transfer to a heated circular jet impinging on a flat surface. Journal of Heat Transfer 112, 608–611.

Lee, J., Lee, S.J., 2000. The effect of nozzle configuration on stagnation region heat transfer enhancement of axisymmetric jet impingement. International Journal of Heat and Mass Transfer 43, 3497–3509.

Lytle, D., Webb, B.W., 1994. Air jet impingement heat transfer at low nozzle-plate spacings. International Journal of Heat and Mass Transfer 37, 1687–1697.

Moller, P.S., 1963. Radial flow without swirl between parallel disks. Aeronautical Quarterly 14, 163–186.

Nakabayashi, K., Ichikawa, T., Morinishi, Y., 2002. Size of annular separation bubble around the inlet corner and viscous flow structure between two parallel disks. Experiments in Fluids 32, 425–433.

Obot, N.T., Douglas, W.J.M., Mujumdar, A.S., 1983. Effect of semi-confinement on impingement heat transfer. In: Proceedings of the Seventh International Heat Transfer Conference. Hemisphere, Washington, DC, pp. 395–400.

Yan, X., Baughn, J.W., Mesbah, M., 1992. The effect of Reynolds number on the heat transfer distribution from a flat plate to an impinging jet. Fundamental and Applied Heat Transfer Research for Gas Turbine Engine, ASME, 1–7.